Neutral Higgs Effects on Rare Decay $B\to X_s l^+l^-$ in the T2HDM*

LÜ Lin-Xia[1,2;1)] XIAO Zhen-Jun[1;2)]

1 (Department of Physics and Institute of Theoretical Physics, Nanjing Normal University, Nanjing 210097, China)
2 (Department of Physics, Nanyang Teacher's College, Nanyang 473061, China)

Abstract We calculate the new physics contributions to the branching ratios of the rare decays $B\to X_s l^+l^-$ $(l=e,\mu)$ induced by neutral Higgs bosons loop diagrams in the top quark two-Higgs-doublet model (T2HDM). From the numerical calculations, we find that (a) the neutral Higgs boson's correction to $B\to X_s l^+l^-$ decays interferes constructively with its standard model counterpart, but small in magnitude; (b) the neutral Higgs contributions to the branching ratio of $B\to X_s l^+l^-$ decay can be neglected safely if their masses are larger than 100GeV and $\tan\beta\leqslant 40$.

Key words two-Higgs-doublet model, neutral Higgs bosons, semileptonic decays, branching ratio

1 Introduction

Flavor changing neutral current (FCNC) induced B-meson rare decays occurred only at the loop level in the Standard Model (SM) and the fact that their branching ratios are tiny seems to be confirmed by the present experimental data. Since FCNC processes strongly depend on virtually exchanged particles, they provide a test of the SM and strong constraints on the parameter space of new physics models beyond the SM.

Among various rare B meson decay modes, $B\to X_s\gamma$ decay has received resounding reception in the interested theoretical physics community. From the $B\to X_s\gamma$ decay, only the magnitude of $C_{7\gamma}$ instead of its sign can be constrained by the relevant data. Recently in Ref. [1], the authors investigated the branching ratio $Br(B\to X_s l^+l^-)$ in the Standard Model or with the reversed sign of $C_{7\gamma}$, and found that the recent data prefer a SM-like Wilson coefficient $C_{7\gamma}(m_b)$.

The B-meson semileptonic decays $B\to X_s l^+l^-$ $(l=e,\mu)$ are of special interest because it is amenable to a clean theoretical description, especially for dilepton invariant masses below the charm resonances, namely in the range $1\text{GeV}^2\lesssim m_{ll}^2\lesssim 6\text{GeV}^2$. The calculation of the next-to-next-to-Leading Order (NNLO) QCD corrections in the SM for $B\to X_s l^+l^-$ has been completed[2—6]. These semileptonic decays, on the experimental side, have been measured by Belle and BaBar[7—9]. At the forthcoming LHC-b or the future super B factory experiments, the dilepton invariant mass spectrum will be measured precisely, which will provide strong constraints on the new physics beyond the Standard Model.

In a previous paper[10], we studied the new physics contributions to the $B\to X_s\gamma$ and $B\to X_s l^+l^-$ decays induced by the charge-Higgs loop diagrams, and found that a charge-Higgs boson with a mass lighter

---

Received 25 October 2006, Revised 2 February 2007

* Supported by National Natural Science Foundation of China (10575052) and Specialized Research Fund for the Doctoral Program of Ministry of Education of China (SRFDP) (20050319008)

1) E-mail: lulinxia@email.njnu.edu.cn
2) E-mail: xiaozhenjun@njnu.edu.cn

than 200GeV is clearly excluded by the data, but a charged Higgs boson with a mass around or larger than 300GeV is still allowed. In this paper, we will concentrate on the calculation of new physics contribution to the semileptonic decays $B \to X_s l^+l^-$ ($l=e,\mu$) induced by the loop diagrams involving the neutral-Higgs bosons that appeared in the T2HDM.

This paper is organized as follows. In Section 2, we briefly review the top quark two-Higgs-doublet model, then calculate the new penguin or box diagrams induced by neutral Higgs bosons, extracting out the new physics parts of the Wilson coefficients in the T2HDM and giving the related formulae for branching ratio $Br(B \to X_s l^+l^-)$. In Section 3, we present the numerical results for the branching ratios of the rare decays $B \to X_s l^+l^-$ in the SM and the T2HDM.

2 Rare decays $B\to X_s l^+l^-$ in the T2HDM

In this section, we present the basic theoretical framework of the T2HDM and calculate the new physics contributions to the Wilson coefficients induced by the loop diagrams involving the neutral Higgs bosons.

The new physics model considered here is the T2HDM proposed in Ref. [11] and studied for example in Refs. [10,12—14], which is also a special case of the 2HDM of type III[15]. The top quark is assigned a special status by coupling it to one Higgs doublet that gets a large VEV, whereas all the other quarks are coupled only to the other Higgs doublet whose VEV is much smaller. As a result, $\tan\beta$ is naturally large in this model.

The Yukawa interaction of the T2HDM can be written as follows[11]:

$$\begin{aligned}\mathscr{L}_{\rm Y} = & -\overline{L}_{\rm L}\phi_1 E l_{\rm R} - \overline{Q}_{\rm L}\phi_1 F d_{\rm R} - \overline{Q}_{\rm L}\widetilde{\phi}_1 G\boldsymbol{1}^{(1)}u_{\rm R} - \\ & \overline{Q}_{\rm L}\widetilde{\phi}_2 G\boldsymbol{1}^{(2)}u_{\rm R} + {\rm H.c.}\end{aligned} \tag{1}$$

where ϕ_i $(i=1,2)$ are the two Higgs doublets with $\widetilde{\phi}_i = {\rm i}\tau_2\phi_i^*$; and E, F, G are the generation space 3×3 matrices; $Q_{\rm L}$ and $L_{\rm L}$ are 3-vector of the left-handed quark and lepton doublets; $\boldsymbol{1}^{(1)} \equiv {\rm diag}(1,1,0)$; $\boldsymbol{1}^{(2)} \equiv {\rm diag}(0,0,1)$ are the two orthogonal projection operators onto the first two and the third families respectively.

The Yukawa couplings for quarks are of the form[11]

$$\begin{aligned}\mathscr{L}_{\rm Y} = & -\sum_{\rm D=d,s,b} m_{\rm D}\bar{D}D - \sum_{\rm U=u,c,t} m_{\rm U}\bar{U}U - \\ & \sum_{\rm D=d,s,b}\frac{m_{\rm D}}{v}\bar{D}D[H^0-\tan\beta h^0] - \\ & {\rm i}\sum_{\rm D=d,s,b}\frac{m_{\rm D}}{v}\bar{D}\gamma_5 D[G^0-\tan\beta A^0] - \\ & \frac{m_{\rm u}}{v}\bar{u}u[H^0-\tan\beta h^0] - \frac{m_{\rm c}}{v}\bar{c}c[H^0-\tan\beta h^0] - \\ & \frac{m_{\rm t}}{v}\bar{t}t[H^0+\cot\beta h^0] + \\ & {\rm i}\frac{m_{\rm u}}{v}\bar{u}\gamma_5 u[G^0-\tan\beta A^0] + \\ & {\rm i}\frac{m_{\rm c}}{v}\bar{c}\gamma_5 c[G^0-\tan\beta A^0] + \\ & {\rm i}\frac{m_{\rm t}}{v}\bar{t}\gamma_5 t[G^0+\cot\beta A^0] + \\ & \frac{g}{\sqrt{2}M_{\rm W}}\{-\overline{U}_{\rm L}Vm_{\rm D}D_{\rm R}[G^+-\tan\beta H^+] + \\ & \overline{U}_{\rm R}m_{\rm U}VD_{\rm L}[G^+-\tan\beta H^+] + \\ & \overline{U}_{\rm R}\Sigma^\dagger VD_{\rm L}[\tan\beta+\cot\beta]H^+ + {\rm h.c.}\}\ ,\end{aligned} \tag{2}$$

where $G^\pm$ and G^0 are Goldstone bosons, $H^\pm$ are charged Higgs bosons, while the CP-even (H^0,h^0) and CP-odd A^0 are the so-called neutral Higgs bosons. Here $M_{\rm U}$ and $M_{\rm D}$ are the diagonal up- and down-type mass matrices, V is the usual Cabibbo-Kobayashi-Maskawa (CKM) matrix and $\Sigma \equiv M_{\rm U}U_{\rm R}^\dagger\boldsymbol{1}^{(2)}U_{\rm R}$. $U_{\rm R}^\dagger$ is the unitary matrix which diagonalizes the right-handed up-type quarks as defined in Ref. [12].

The effective hamiltonian inducing the transition $b\to sl^+l^-$ at the scale μ has the following structure[16]:

$$\mathscr{H} = -\frac{4G_{\rm F}}{\sqrt{2}}V_{\rm ts}^*V_{\rm tb}\sum_{i=1}^{10}[C_i(\mu)\mathscr{O}_i(\mu)+C_{Q_i}(\mu)Q_i(\mu)], \tag{3}$$

where $C_i(\mu)$, $C_{Q_i}(\mu)$ are the Wilson coefficients at the renormalization point $\mu = m_{\rm W}$, $\mathscr{O}_i$'s $(i=1,\cdots,10)$ are the operators in the SM and are the same as those given in Ref. [2], and Q_i's come from exchanging the neutral Higgs bosons in T2HDM and have been given in Ref. [16]. $G_{\rm F}=1.16639\times10^{-5}{\rm GeV}^{-2}$ is the Fermi coupling constant, and $V_{\rm ts}^{*}V_{\rm tb}$ is the CKM factor. We work in the approximation where the combination $(V_{\rm us}^{*}V_{\rm ub})$ of the CKM matrix elements is neglected. The top-quark and charm-quark contributions are added up with the results in the summed form.

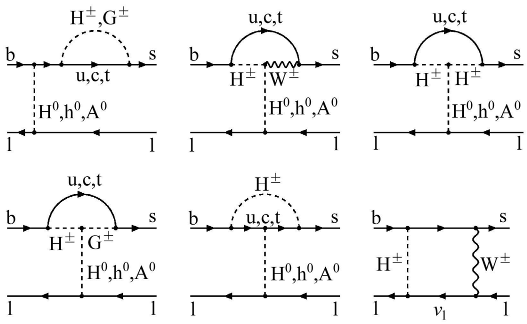

Fig. 1. The typical Feynman diagrams for the decay $\rm B\to X_s l^+l^-$ when the new physics contributions from the loops involving the neutral Higgs bosons in T2HDM. The box diagram in the lower right corner is an example of the diagrams involving the charged Higgs boson.

In the framework of the SM, the rare decays $\rm B\to X_s l^+l^-$ proceed through loop diagrams and are of forth order in the weak coupling. The dominant contributions to this decay come from the W box and Z penguin diagrams. The corresponding one-loop diagrams in the SM were evaluated long time ago and can be found for example in Refs. [17, 18].

In the T2HDM, the $\rm B\to X_s l^+l^-$ decays proceed also via additional loops involving the charged and/or neutral Higgs bosons exchanges. In Ref. [10], we have given a detailed derivation of the lengthy expressions of the T2HDM corrections to the relevant Wilson coefficients induced by the loop diagrams involving the charged Higgs bosons. Here we first consider the neutral Higgs bosons contributions to the Wilson coefficients.

At the high energy scale $\mu_{\rm W}\sim M_{\rm W}$, the leading contributions to C_{Q_i} come from the diagrams in Fig. 1. By calculating the Feynman diagrams, we find analytically that

$$
\begin{aligned}
C_{Q_1}(M_{\rm W}) = &-f_{\rm ac}\sum_{\rm i=c,t}\kappa^{\rm is}\Bigg\{\frac{m_{\rm i}^2}{m_{\rm h^0}^2}\left(-\tan^2\beta+\frac{(\Sigma^{\rm T}V^*)_{\rm is}}{m_{\rm i}V_{\rm is}^*}(\tan^2\beta+1)\right)\bar{B}_0(y_{\rm i})-\frac{m_{\rm i}^2}{m_{\rm h^0}^2}\bar{B}_0(x_{\rm i})-\\
&\frac{M_{\rm W}^2}{m_{\rm h^0}^2}\Bigg[x_{\rm i}\left(-1+\frac{(\Sigma^{\dagger}V)_{\rm ib}}{m_{\rm i}V_{\rm ib}}(\cot^2\beta+1)\right)\left(2\bar{C}_{01}(x_{\rm i},y_{\rm i},x_{\rm H^+})-\bar{C}_{11}(x_{\rm i},y_{\rm i},x_{\rm H^+})\right)+\\
&\frac{m_{\rm b}^2}{M_{\rm W}^2}\left(2\bar{C}_{11}(x_{\rm i},y_{\rm i},x_{\rm H^+})-\bar{C}_{22}(x_{\rm i},y_{\rm i},x_{\rm H^+})\right)+\bar{C}_{21}(x_{\rm i},y_{\rm i},x_{\rm H^+})\Bigg]+\\
&x_{\rm i}\left(\frac{m_{\rm H^+}^2}{m_{\rm h^0}^2}-1\right)\left[\left(-1+\frac{(\Sigma^{\dagger}V)_{\rm ib}}{m_{\rm i}V_{\rm ib}}(\cot^2\beta+1)\right)\bar{C}_{11}(x_{\rm i},y_{\rm i},x_{\rm H^+})+\bar{C}_{01}(x_{\rm i},y_{\rm i},x_{\rm H^+})\right]+\\
&\frac{m_{\rm i}^2(2m_{\rm H^+}^2+m_{\rm H^0}^2-2m_{\rm h^0}^2)}{m_{\rm H^+}^2m_{\rm H^0}^2}\left(-1+\frac{(\Sigma^{\rm T}V^*)_{\rm is}}{m_{\rm i}V_{\rm is}^*}(\cot^2\beta+1)\right)\times\\
&\left[\left(-1+\frac{(\Sigma^{\dagger}V)_{\rm ib}}{m_{\rm i}V_{\rm ib}}(\cot^2\beta+1)\right)C_{11}(y_{\rm i})+C_{01}(y_{\rm i})\right]+\\
&\frac{m_{\rm i}^2Q'_{\rm h^0}\tan\beta}{m_{\rm h^0}^2}\Bigg[y_{\rm i}\left(-1+\frac{(\Sigma^{\rm T}V^*)_{\rm is}}{m_{\rm i}V_{\rm is}^*}(\cot^2\beta+1)\right)\times\\
&\left(C''_{01}(y_{\rm i})-\frac{m_{\rm b}^2}{m_{\rm i}^2}C''_{11}(y_{\rm i})-\frac{1}{y_{\rm i}}C''_{21}(y_{\rm i})\right)+\\
&y_{\rm i}\left(-1+\frac{(\Sigma^{\rm T}V^*)_{\rm is}}{m_{\rm i}V_{\rm is}^*}(\cot^2\beta+1)\right)\left(-1+\frac{(\Sigma^{\dagger}V)_{\rm ib}}{m_{\rm i}V_{\rm ib}}(\cot^2\beta+1)\right)\times\\
&(C''_{01}(y_{\rm i})-2C''_{11}(y_{\rm i}))+\frac{m_{\rm b}^2}{18M_{\rm H^+}^2}\left(-1+\frac{(\Sigma^{\rm T}V^*)_{\rm is}}{m_{\rm i}V_{\rm is}^*}(\cot^2\beta+1)\right)C''_{22}(y_{\rm i})\Bigg]-B_{+}(x_{\rm H^+},x_{\rm t})\Bigg\}\ ,
\end{aligned}
\tag{4}
$$

$$
\begin{aligned}
C_{Q_2}(M_{\rm W}) = & f_{\rm ac}\sum_{\rm i=c,t}\kappa^{\rm is}\Bigg\{\frac{m_{\rm i}^2}{m_{\rm A^0}^2}\left[\left(-\tan^2\beta+\frac{(\Sigma^{\rm T}V^*)_{\rm is}}{m_{\rm i}V^*_{\rm is}}(\tan^2\beta+1)\right)\bar{B}_0(y_{\rm i})-\bar{B}_0(x_{\rm i})\right]- \\
& \frac{M_{\rm W}^2}{m_{\rm A^0}^2}\left[x_{\rm i}\left(-1+\frac{(\Sigma^\dagger V)_{\rm ib}}{m_{\rm i}V_{\rm ib}}(\cot^2\beta+1)\right)\left(2\bar{C}_{01}(x_{\rm i},y_{\rm i},x_{\rm H^+})-\bar{C}_{11}(x_{\rm i},y_{\rm i},x_{\rm H^+})\right)+\right. \\
& \left.\frac{m_{\rm b}^2}{M_{\rm W}^2}\left(2\bar{C}_{11}(x_{\rm i},y_{\rm i},x_{\rm H^+})-\bar{C}_{22}(x_{\rm i},y_{\rm i},x_{\rm H^+})\right)+\bar{C}_{21}(x_{\rm i},y_{\rm i},x_{\rm H^+})\right]+ \\
& x_{\rm i}\left(\frac{m_{\rm H^+}^2}{m_{\rm A^0}^2}-1\right)\left[\left(-1+\frac{(\Sigma^\dagger V)_{\rm ib}}{m_{\rm i}V_{\rm ib}}(\cot^2\beta+1)\right)\bar{C}_{11}(x_{\rm i},y_{\rm i},x_{\rm H^+})+\bar{C}_{01}(x_{\rm i},y_{\rm i},x_{\rm H^+})\right]- \\
& \frac{m_{\rm i}^2Q'_{\rm A^0}\tan\beta}{m_{\rm A^0}^2}\left[y_{\rm i}\left(-1+\frac{(\Sigma^{\rm T}V^*)_{\rm is}}{m_{\rm i}V^*_{\rm is}}(\cot^2\beta+1)\right)\left(C''_{01}(y_{\rm i})+\frac{m_{\rm b}^2}{m_{\rm i}^2}C''_{11}(y_{\rm i})+\frac{1}{y_{\rm i}}C''_{21}(y_{\rm i})\right)+\right. \\
& y_{\rm i}\left(-1+\frac{(\Sigma^{\rm T}V^*)_{\rm is}}{m_{\rm i}V^*_{\rm is}}(\cot^2\beta+1)\right)\left(-1+\frac{(\Sigma^\dagger V)_{\rm ib}}{m_{\rm i}V_{\rm ib}}(\cot^2\beta+1)\right)C''_{01}(y_{\rm i})- \\
& \left.\frac{m_{\rm b}^2}{18M_{\rm H^+}^2}\left(-1+\frac{(\Sigma^{\rm T}V^*)_{\rm is}}{m_{\rm i}V^*_{\rm is}}(\cot^2\beta+1)\right)C''_{22}(y_{\rm i})\right]-B_+(x_{\rm H^+},x_{\rm t})\Bigg\}\,,
\end{aligned}
\tag{5}
$$

$$C_{Q_3}(M_{\rm W}) = \frac{m_{\rm b}e^2}{m_{\rm l}g_{\rm s}^2}(C_{Q_1}(M_{\rm W})+C_{Q_2}(M_{\rm W})), \tag{6}$$

$$C_{Q_4}(M_{\rm W}) = \frac{m_{\rm b}e^2}{m_{\rm l}g_{\rm s}^2}(C_{Q_1}(M_{\rm W})-C_{Q_2}(M_{\rm W})), \tag{7}$$

$$C_{Q_i}(M_{\rm W}) = 0, \quad \text{for} \quad i=5,\cdots,10, \tag{8}$$

where $f_{\rm ac} = \frac{m_{\rm b}m_{\rm l}\tan^2\beta}{4M_{\rm W}^2\sin^2\theta_{\rm W}}$, $\kappa^{\rm is} = -V_{\rm ib}V^*_{\rm is}/(V_{\rm tb}V^*_{\rm ts})$, $x_{\rm H^+} = m_{\rm H^+}^2/M_{\rm W}^2$, $x_{\rm i} = m_{\rm i}^2/M_{\rm W}^2$, $y_{\rm i} = m_{\rm i}^2/m_{\rm H^+}^2$, and $Q'_{\rm A^0} = Q'_{\rm h^0} = \tan\beta(-\cot\beta)$ for $c(t)$ quark. The one-loop integral functions that appeared in $C_{Q_1}(M_{\rm W})$ and $C_{Q_2}(M_{\rm W})$ can be written as

$$
\begin{aligned}
\bar{B}_0(y) = & 1+\frac{y}{1-y}\ln[y]\,, \\
B_+(x,y) = & \frac{y}{x-y}\left(\frac{\ln[x]}{1-x}-\frac{\ln[y]}{1-y}\right), \\
C_{01}(y) = & \frac{1}{1-y}+\frac{y}{(1-y)^2}\ln[y]\,, \\
C_{11}(y) = & \frac{1-3y}{4(1-y)^2}-\frac{y^2}{2(1-y)^3}\ln[y]\,,
\end{aligned}
\tag{9}
$$

$$
\begin{aligned}
C''_{01}(y) = & -\frac{1}{1-y}-\frac{1}{(1-y)^2}\ln[y]\,, \\
C''_{11}(y) = & \frac{y-3}{4(1-y)^2}-\frac{1}{2(1-y)^3}\ln[y]\,, \\
C''_{21}(y) = & \frac{3-y}{2(1-y)}+\frac{1}{(1-y)^2}\ln[y]\,, \\
C''_{22}(y) = & \frac{-11+7y-2y^2}{(1-y)^3}-\frac{6}{(1-y)^4}\ln[y],
\end{aligned}
$$

$$
\begin{aligned}
\bar{C}_{01}(x,y,z) = & \frac{y\ln[x]-x\ln[y]-\ln[z]}{(1-x)(1-y)(1-z)}\,, \\
\bar{C}_{11}(x,y,z) = & -\frac{1}{2(1-y)(1-z)}-\frac{y^2}{2(1-x)(1-y)^2}\ln[y]-\frac{1}{2(1-x)(1-z)^2}\ln[z]\,, \\
\bar{C}_{21}(x,y,z) = & \frac{3}{2}-\frac{xy}{(1-x)(1-y)}\ln[y]+\frac{1}{(1-x)(1-z)}\ln[z]\,, \\
\bar{C}_{22}(x,y,z) = & \frac{-3x+5y+z-3}{6(1-y)^2(1-z)^2}+\frac{y^3}{3(1-x)(1-y)^3}\ln[y]-\frac{1}{3(1-x)(1-z)^3}\ln[z]\,.
\end{aligned}
\tag{10}
$$

Neglecting the strange quark mass, the effective Hamiltonian Eq. (3) leads to the following matrix element for the rare decays $B\to X_s l^+l^-$

$$
\begin{aligned}
\mathscr{M} = & \frac{\alpha_{\rm em}G_{\rm F}}{2\sqrt{2}\pi}V_{\rm tb}V^*_{\rm ts}\Big\{-2\widetilde{C}^{\rm eff}_{7\gamma}\frac{m_{\rm b}}{q^2}\bar{s}{\rm i}\sigma_{\mu\nu}p_\nu(1+\gamma_5)b\bar{l}\gamma_\mu l+ \\
& \widetilde{C}^{\rm eff}_{9V}\bar{s}\gamma_\mu(1-\gamma_5)b\bar{l}\gamma_\mu l+\widetilde{C}^{\rm eff}_{10A}\bar{s}\gamma_\mu(1-\gamma_5)b\bar{l}\gamma_\mu\gamma_5 l+ \\
& C_{Q_1}\bar{s}(1+\gamma_5)b\bar{l}l+C_{Q_2}\bar{s}(1+\gamma_5)b\bar{l}\gamma_5 l\Big\}.
\end{aligned}
\tag{11}
$$

with q the momentum transfer.

The Wilson coefficients can be evolved from the electroweak scale $\mu_{\rm W}\sim M_{\rm W}$ down to the low-energy scale $\mu \sim m_{\rm b}$, according to the renormalization group equation[5]. The mixing of the operators $\mathscr{O}_i$ $(i=1,2,\cdots,10)$ in the SM has been studied and the anomalous dimension matrix (ADM) has been given in Refs. [3—6]. Neglecting the mixing between $\mathscr{O}_i(i=1,2,\cdots,10)$ and $Q_i(i=1,2,\cdots,10)$, the effective Wilson coefficients including the charged Higgs bosons contributions at the low scale $\mu=m_{\rm b}$ can be found in Ref. [10].

The operators $\mathscr{O}_i(i=1,\cdots,10)$ and $Q_i(i=3,\cdots,10)$ do not mix into Q_1 and Q_2 and there is no mixing between Q_1 and Q_2[19]. Therefore, the evolution of the Wilson coefficients C_{Q_1} and C_{Q_2} is

$$C_{Q_i}(\mu_{\rm b})=\eta^{-12/23}C_{Q_i}(M_{\rm W})\,, \tag{12}$$

where $\eta=\alpha_s(M_{\rm W})/\alpha_s(\mu_{\rm b})$.

In order to eliminate the large uncertainties due to the factor $m_{\rm b}^5$ and the CKM elements appearing in the decay width for $\rm B\to X_s l^+l^-$, it has become customary to normalize the decay to the semileptonic decay rate. The integrated branching ratio in low-q^2 region can be written as[6, 20]

$$Br_{\rm ll}=Br(\bar{\rm B}\to {\rm X_c l\nu})\int_{\hat{s}_{\rm a}}^{\hat{s}_{\rm b}}R(\hat{s})\ , \tag{13}$$

where $\hat{s}=q^2/m_{\rm b}^2$ with $\hat{s}_{\rm a}=1/m_{\rm b}^2$ and $\hat{s}_{\rm b}=6/m_{\rm b}^2$, $R(\hat{s})$ is the differential decay rate for the decay $\rm B\to X_s l^+l^-$ and has been derived in Ref. [16]

$$R(\hat{s})\ \equiv\ \frac{\frac{\rm d}{{\rm d}\hat{s}}\Gamma({\rm b\to s l^+l^-})}{\Gamma({\rm b\to ce\bar{\nu}})}=\frac{\alpha_{\rm em}^2}{4\pi^2}\left|\frac{V_{\rm ts}^*V_{\rm tb}}{V_{\rm cb}}\right|^2\times$$
$$\frac{(1-\hat{s})^2}{f(z)\kappa(z)}\left(1-\frac{4r}{\hat{s}}\right)^{1/2}D(\hat{s})\ , \tag{14}$$

where

$$\begin{aligned}D(\hat{s})\ =\ &4|\widetilde{C}_7^{\rm eff}|^2\left(1+\frac{2r}{\hat{s}}\right)\left(1+\frac{2}{\hat{s}}\right)+\\ &|\widetilde{C}_9^{\rm eff}|^2\left(1+\frac{2r}{\hat{s}}\right)(1+2\hat{s})+\\ &|\widetilde{C}_{10}^{\rm eff}|^2\left(1-8r+2\hat{s}+\frac{2r}{\hat{s}}\right)+\\ &12{\rm Re}(\widetilde{C}_7^{\rm eff}\widetilde{C}_9^{\rm eff*})\left(1+\frac{2r}{\hat{s}}\right)+\\ &\frac{3}{2}|C_{Q_1}|^2(\hat{s}-4r)+\frac{3}{2}|C_{Q_2}|^2\hat{s}+\\ &6{\rm Re}(\widetilde{C}_{10}^{\rm eff}C_{Q_2}^*)r^{1/2}\ .\end{aligned} \tag{15}$$

Here $r=m_{\rm l}^2/m_{\rm b}^2$, $z=m_{\rm c}/m_{\rm b}$, $f(z)=1-8z^2+8z^6-z^8-24z^4\ln z$ is the phase-factor, and $\kappa(z)\simeq 1-\frac{2\alpha_s(\mu)}{3\pi}\left[\left(\pi^2-\frac{31}{4}\right)(1-z)^2+\frac{3}{2}\right]$ is the single gluon QCD correction to the $\rm b\to ce\bar{\nu}$ decay.

3 Numerical result

In numerical calculations, we will use the following input parameters

$$\begin{aligned}&m_{\rm d}=5.4{\rm MeV},\ m_{\rm s}=150{\rm MeV},\ m_{\rm b}=4.6{\rm GeV},\\ &m_{\rm c}=1.4{\rm GeV},\quad \overline{m}_{\rm t}(m_{\rm t})=165.9{\rm GeV},\\ &m_{\rm B_d}=5.279{\rm GeV},\quad m_{\rm B_s}=5.367{\rm GeV},\\ &A=0.853,\quad \lambda=0.225,\quad \bar{\rho}=0.20\pm0.09,\\ &\bar{\eta}=0.33\pm0.05,\end{aligned} \tag{16}$$

where A, λ, $\bar{\rho}$ and $\bar{\eta}$ are Wolfenstein parameters of the CKM mixing matrix.

From the data of the radiative decay $\rm B\to X_s\gamma$ and $\rm B^0-\bar{B}^0$ mixing, we found strong constraints on the parameter space of the T2HDM[10]. Here we will consider these constraints in our choice for the free parameters of the T2HDM.

On the experimental side, the average of the measured branching ratios of $\rm B\to X_s l^+l^-$ $(\rm l=e,\mu)$ for the low dilepton invariant mass region $(1{\rm GeV}^2<m_{\rm ll}^2\equiv q^2<6{\rm GeV}^2)$ as given in Ref. [1] is

$$Br({\rm B\to X_s l^+l^-})=(1.60\pm0.51)\times10^{-6}. \tag{17}$$

At NNLO level, the SM prediction after integrating over the low-q^2 region reads

$$\begin{aligned}Br({\rm B\to X_s l^+l^-})=&\big(1.58\pm0.08|_{m_{\rm t}}\pm0.07|_{\mu_{\rm b}}\pm\\ &0.04|_{\rm CKM}\pm0.06|_{m_{\rm b}}+0.18|_{\mu_{\rm W}}\big)\times10^{-6}=\\ &(1.58\pm0.13+0.18|_{\mu_{\rm W}})\times10^{-6}\ .\end{aligned} \tag{18}$$

where the errors show the uncertainty of input parameters of $m_{\rm t}$, A, $\bar{\rho}$, $\bar{\eta}$ and $m_{\rm b}$, and for $m_{\rm b}/2\leqslant\mu_{\rm b}\leqslant2m_{\rm b}$. The last error corresponds to the choice of $\mu_{\rm W}=120{\rm GeV}$, instead of $\mu_{\rm W}=M_{\rm W}$. Since here we focus on the new physics corrections to the branching ratios of $\rm B\to X_s l^+l^-$ decay, we will take $\mu_{\rm W}=M_{\rm W}$ in the following unless stated otherwise.

The new physics corrections to the branching ratio of $\rm B\to X_s l^+l^-(l=e,\mu)$ in T2HDM are shown in Fig. 2 and Fig. 3. The band between two horizontal dot lines refers to the data within 1σ error: $Br(B\to X_s l^+l^-)=(1.60\pm0.51)\times10^{-6}$; while the solid line corresponds to the central value of the SM prediction at NNLO level: $Br(B\to X_s l^+l^-)=1.58\times10^{-6}$.

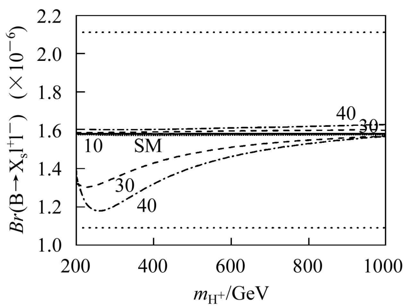

Fig. 2. Plots of the branching ratios of $B\to X_s l^+l^-$ vs the mass m_{H^+} in the SM and T2HDM for $\delta=0°$, $m_{H^0}=160$GeV, $m_{h^0}=115$GeV, $m_{A^0}=120$GeV and for $\tan\beta=10$, $\tan\beta=30$, $\tan\beta=40$, respectively.

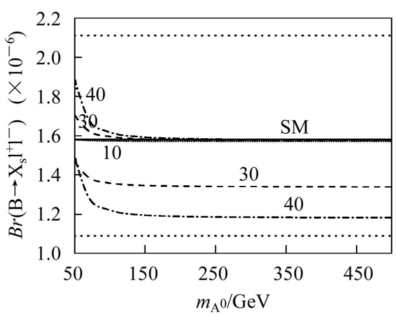

Fig. 3. Plots of the branching ratio of $B\to X_s l^+l^-$ vs the mass m_{A^0} for $\delta=0°$, $m_{H^+}=300$GeV, $m_{H^0}=160$GeV, $m_{h^0}=115$GeV, and for $\tan\beta=10$, 30, 40, respectively.

In Fig. 2, the dot-dashed and dashed curve little above the solid line (SM prediction) are the T2HDM predictions for $\tan\beta=40$ and 30 respectively, when only the new physics contributions from neutral Higgs bosons are taken into account (the case A), while the dot-dashed and dashed curves below the solid line (SM prediction) show the corresponding T2HDM predictions when the new physics contributions from both the neutral and charged Higgs bosons are included (the case B). For $\tan\beta\leqslant10$, the new physics contributions in both case A and B are always very small and can be neglected safely.

In Fig. 3, we show the the m_{A^0} dependence of $Br(B\to X_s l^+l^-)$ for $\delta=0°$, $m_{H^+}=300$GeV, $m_{H^0}=160$GeV, $m_{h^0}=115$GeV, and for $\tan\beta=10$, 30, 40, respectively. Again, the dot-dashed and dashed curve little above (below) the central solid line are the T2HDM predictions for the case A (case B) and for $\tan\beta=40$ and 30 respectively. For $\tan\beta\leqslant10$, the curves in the T2HDM cannot be separated with the solid line (SM prediction).

For the CP-even neutral Higgs boson H^0 and h^0, we have the similar results. The neutral Higgs bosons contributions to the decays $B\to X_s l^+l^-$ are always very small if their masses are heavier than 100GeV as suggested by the direct experimental searches.

To summarize, we have calculated the new physics contributions to the rare B meson decays $B\to X_s l^+l^-$ induced by the loop diagrams involving the neutral or charged Higgs bosons in the top-quark two-Higgs-doublet model, and compared the theoretical predictions in the SM and the T2HDM with currently available data. From the numerical results and the figures, we found the following points.

(i) The neutral Higgs contributions to the branching ratio $Br(B\to X_s l^+l^-)$ interfere constructively with their SM counterparts, but small in magnitude. The charged Higgs, however, can provide large new physics contribution to both $B\to X_s\gamma$ and $B\to X_s l^+l^-$ decays.

(ii) The neutral Higgs contributions to the branching ratio of $B\to X_s l^+l^-$ decay can be neglected safely if their masses are larger than 100GeV and $\tan\beta\leqslant40$.

(iii) Within the considered parameter space of the T2HDM, the theoretical predictions for $Br(B\to X_s l^+l^-)$ always agree well with the measured value within one standard deviation.

References

1 Gambino P, Haisch U, Misiak M. Phys. Rev. Lett. , 2005, **94**: 061803

2 Bobeth C, Misiak M, Urban J. Nucl. Phys. , 2000, **B574**: 291—330

3 Asatryan H H, Asatrian H M, Greub C et al. Phys. Rev. , 2002, **D65**: 074004; Asatryan H H, Asatrian H M, Greub C et al. Phys. Rev. , 2002, **D66**: 034009; Ghinculov A, Hurth T, Isidori G et al. Nucl. Phys. , 2003, **B648**: 254—276; Asatrian H M, Bieri K, Greub C et al. Phys. Rev. , 2002, **D66**: 094013

4 Gambino P, Gorbahn M, Haisch U. Nucl. Phys. , 2003, **B673**: 238—262

5 Gorbahn M, Haisch U. Nucl. Phys. , 2005, **B713**: 291

6 Bobeth C, Gambino P, Gorbahn M et al. JHEP, 2004, **0404**: 071

7 Abe K et al (Belle Collaboration). Phys. Rev. Lett. , 2002, **88**: 021801; Aubert B et al (BaBar Collaboration). Phys. Rev. Lett. , 2002, **88**: 241801

8 Aubert B et al (BaBar Collaboration). Phys. Rev. Lett. , 2004, **93**: 081802

9 Iwasaki M et al (Belle Collaboration). Phys. Rev. , 2005, **D72**: 092005

10 XIAO Z J, LÜ L X. Phys. Rev. , 2006, **D74**: 034016

11 Das A, Kao C. Phys. Lett. , 1996, **B372**: 106—112

12 Kiers K, Soni A, WU G H. Phys. Rev. , 1999, **D59**: 096001; WU G H, Soni A. Phys. Rev. , 2000, **D62**: 056005

13 Kiers K, Soni A, WU G H. Phys. Rev. , 2000, **D62**: 116004

14 LÜ L X, XIAO Z J. Commun. Theor. Phys., 2007, **47**: 1099

15 HOU W S. Phys. Lett. , 1992, **B296**: 179; Luke M, Savage M J. Phys. Lett. , 1993, **B307**: 387

16 DAI Y B, HUANG C S, HUANG H W. Phys. Lett. , 1997, **B390**: 257; 2001, **B513**: 429; HUANG C S, LIAO W, YAN Q S et al. Phys. Rev. , 2001, **D63**: 114021; 2001, **D64**: 059902

17 Inami T, Lim C S. Prog. Theor. Phys, 1981, **65**: 297—314; 1981, **65**: 1772

18 Misiak M. Nucl. Phys. , 1993, **B393**: 23

19 HUANG C S. Commun. Theor. Phys., 1983, **2**: 1265

20 Bobeth C, Buras A J, Früger F et al. Nucl. Phys. , 2002, **B630**: 87—131; Bobeth C, Buras A J, Ewerth T. Nucl. Phys. , 2005, **B713**: 522—554

在T2HDM模型中中性希格斯粒子对$\mathrm{B}\rightarrow \mathrm{X_s l^+ l^-}$衰变过程的影响*

吕林霞[1,2;1)] 肖振军[1;2)]

1 (南京师范大学物理科学与技术学院 南京 210097)
2 (南阳师范学院物理系 南阳 473061)

摘要 在T2HDM模型中计算了中性希格斯粒子圈图对稀有衰变过程$\mathrm{B}\rightarrow \mathrm{X_s l^+ l^-}$的贡献. 通过计算发现: (a) 中性希格斯粒子对衰变过程$\mathrm{B}\rightarrow \mathrm{X_s l^+ l^-}$的修正能够增强其标准模型的预言, 但增幅很小; (b) 在中性希格斯玻色子的质量大于100GeV和$\tan\beta < 40$的情况下, 中性希格斯粒子对稀有衰变过程$\mathrm{B}\rightarrow \mathrm{X_s l^+ l^-}$的分支比的贡献可忽略.

关键词 双希格斯模型 中性希格斯玻色子 半轻衰变 分支比

2006 – 10 – 25 收稿, 2007 – 02 – 02 收修改稿
* 国家自然科学基金(10575052)和国家教育部博士点科研基金(20050319008)资助
1) E-mail: lulinxia@email.njnu.edu.cn
2) E-mail: xiaozhenjun@njnu.edu.cn